Enhanced Operational Stability through Interfacial Modification by Active Encapsulation of Perovskite Solar Cells

Sudeshna Ghosh[1], Roja Singh[2], Anand S. Subbiah[2], Pablo P. Boix[3], Ivan Mora-Sero[4] and Shaibal K Sarkar[2]

[1] *Center of Research in Nanotechnology and Science, Powai, Mumbai 400 076 India*

[2] *Department of Energy Science and Engineering, Indian Institute of Technology Bombay, Powai, Mumbai 400 076 India*

[3] *Institut de Ciència dels Materials, University of Valencia Catedràtic J. Beltran 246980 Paterna, Valencia, Spain*

[4] *Institute of Advanced Materials, Universitat Jaume I, Av. de Vicent Sos Baynat, s/n 12071Castelló de la Plana, Spain*

Corresponding Author

shaibal.sarkar@iitb.ac.in.

Abstract:

Encapsulates are, in general, the *passive* components of any photovoltaic device that provide needed shielding from the externally stimulated degradation. Here we provide comprehensive physical insight depicting a rather non-trivial *active* nature, in contrast to the supposedly passive, ALD grown Al_2O_3 encapsulate layer on the hybrid perovskite ($(FA_{0.83}MA_{0.17})_{0.95}Cs_{0.05}PbI_{2.5}Br_{0.5}$) photovoltaic device having the configuration; glass/FTO/SnO2/perovskite/Spiro-OMeTAD/Au/ (±) Al2O3. By combination of various electrical characterizations techniques, our experimental observations indicate that the ALD chemistry produces considerable enhancement of the electronic conductivity of the spiro-OMeTAD hole transport medium (HTM) resulting in electronic modification of the perovskite/HTM interface. Subsequently, the modified interface provides better hole extraction and lesser ionic accumulation at the interface, resulting in a significant lowering of the *burn-in* decay and nearly unchanged charge transport parameters explicitly under the course of continuous operation. Unlike unencapsulated device, the modified electronic structure in the Al_2O_3 coated device is essentially the principal reason for better performance stability. Data presented in this communication suggests that the ionic accumulation at the spiro-OMeTAD/perovskite interface triggers the device degradation in the uncoated devices that is eventually followed by materials degradation which can be avoided by active encapsulation.

KEYWORDS-Perovskite solar cell, ALD Al_2O_3, Unencapsulated, Encapsulated, S-shape, Interface, Ion-accumulation

Intrinsic[1,2]and the extrinsic[3,4,5,6] routes of degradation are the primary bottleneck that thwart the commercial realization of hybrid perovskite solar cells (PSC). Prevailing measures taken to avoid the extrinsic degradation[7,8] are efficient encapsulate to protect the active device, mainly, from humidity and oxygen.

In this context, recent reports [9,10,11] suggest the applicability of atomic layer deposition (ALD) grown Al_2O_3 layer as a preventive measure against the degradation, leading to improved device performance under diurnal cycles.[12] The surface-limited ingrowth of the as-deposited Al_2O_3 in the spiro-OMeTAD layer during the nucleation period essentially holds the key, that places this technique as an efficient measure for the long-term stability of the device.[13]

In addition to the conventional extrinsic degradation mechanisms, recent studies report factors that can accelerate the degradation process under certain measurement conditions, increasing the induced stress.[14] Factors like duration, periodicity of measurements,[15] and preconditioning conditions[16] also play an important role in the overall device stability. Generally, induced degradation is often (partially) recoverable [17] and is majorly attributed to the inappropriate distribution of the activated ions.[18] However, under continuous operation, these damages collectively initiate a high level of severity resulting in irreversible degradation. Thus, one could find radical differences in device stability when comparing the performance under intermittent and continuous measurement conditions.[19] When the device is under a relaxing condition in the dark, the redistribution of the mobile ions rejuvenates the device.[20] However, under uninterrupted measurement, efficient charge extraction in conjunction with ideal band alignment encourages the device stability.[21,22] Thus, in the absence of external entities, proper band alignment and chemical inactivity of the ionic

species with the charge transport layers are some of the vital issues to ensure the enhanced device stability even under a stressed condition.

We have recently shown [23] that ALD-grown Al_2O_3 on top of the device escalates the shelf life of the device and enhances the device life under continuous illumination. Though the increased shelf life indicates impermeability against ambient constituents, it is interesting to observe favorable modifications of the interfacial characteristics under continuous illumination. In this communication, we unveil unexpected modifications in the perovskite/spiro-OMeTAD interfacial electronic characteristic upon Al_2O_3 coating on top of the device. The conductivity of the HTM improves upon Al_2O_3 ingrowth, a counter-intuitive phenomenon with a beneficial effect in the charge extraction interface. As a result, the "ALD-encapsulation" demotes charge and ion accumulation at the interface, suppressing chemical modification under continuous operation substantially, in comparison to pristine uncoated devices.

Herein, we fabricate PSCs using the extended multi-cation and multi-anion perovskite ($(FA_{0.83}MA_{0.17})_{0.95}Cs_{0.05}PbI_{2.5}Br_{0.5}$) as an active layer with Bilayer SnO_2 and Li-doped spiro-OMeTAD as electron transport layer (ETL) and hole transporting layer (HTL) respectively, as shown in the Figure S1in Supplementary material. ALD-grown Al_2O_3 is deposited on top of the processed device at 75ºC using trimethyl aluminium and water inside a customized flow reactor. The details of the device fabrication and the ALD process parameters are described in Supplementary material (experimental section).

A passive encapsulation effect should be expected from the Al_2O_3 coating, but surprisingly, we report here that the Al_2O_3 encapsulation process also had an active impact on the device's electronic characteristics. Apart from the previously reported long-term stability,[23] the major differences between the pristine and coated devices during the burn-in period essentially justify the improved light induced degradation of the coated sample over the pristine ones, as

shown in the Figure 1a,b. The burn-in decay is most prominent under the short-circuit condition in comparison with open-circuit; hence, we mostly concentrate our discussion here towards short-circuit conditions (J_{SC}). However, for comparison, the measurements under open circuit conditions (V_{OC}) are also depicted in Figure S2 in Supplementary material. It is also worth mentioning that, under intermittent measurements where the device undergoes relaxation between successive measurements; there is little difference in the photovoltaic device parameters between these competitive devices as shown in Figure S3 in Supplementary material.[24] To better understand the changes of electronic nature that the device undergoes during the burn-in period, we constantly measured the J_{SC} for the first three hours while intermittently recorded J-V sweep (both forward/reverse direction and under light/dark condition) along with electrochemical impedance spectroscopy (EIS) measurements. Experimental details on the intermittent measurement procedure are further briefed in the Supplementary material.

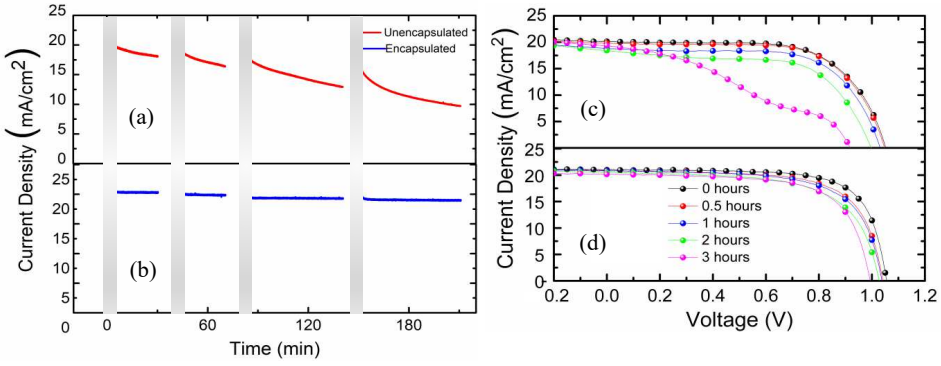

FIG. 1. J_{SC} vs. time for (a) unencapsulated and (b) encapsulated devices along with intermittent J-V (Forward direction) for (c) unencapsulated and (d) encapsulated devices measured at 0, 30 min,60 min,120 min and 180 min. The grey section represents the time regime in which some other experiments are done as described in the experimental section. In Figure 1(a) sharp decrease in current density observed with time in unencapsulated devices whereas in 1(b) no reduction in current density is visible in encapsulated devices. Along with J_{SC} vs time intermittent light J-V of unencapsulated devices shows a visible decrement of FF resulting in a kink (S-shape) formation. On the flipside, no such decrement is observed in intermittent J-V of encapsulated devices.

The shorter time interval in which the devices underwent considerable loss in efficiency is of specific interest, past that the coated device retained a stable performance for up to 100 hours while the pristine devices continue degrading.[23] The evolution of J_{SC} with time is depicted in Figures 1a and 1b for pristine and encapsulated devices respectively. The pristine devices exhibit a sharp decline in the short-circuit current (J_{SC}) over time, where the J_{SC} dropped to 48% of its initial value (20 mA/cm^2 to 9.70 mA/cm^2) within a span of 3 hours (180min). In contrast, the encapsulated cells retained almost 92% of the initial value by the end of 3 hours (180min) (20.7 mA/cm^2 to 19 mA/cm^2). J-V characteristics of the pristine and encapsulated device are measured intermittently to follow the individual device parameters during the continuous J_{SC} measurements, as shown in Figure 1c, d. Though we observed slight changes in V_{OC} and especially in FF from the intermittent J-V characteristics of the encapsulated device, the pristine unencapsulated devices, in contrast, display a significant degradation of the J-V characteristics.

Beyond the decrease in the J_{SC} and V_{OC}, a significant reduction in the fill-factor is clearly observed, as parametrically depicted in Figure S4in Supplementary material. The striking difference is the unprecedented appearance of the S-shape kink (after 3 hours (180 min) here, but typically varies with sample) in the pristine devices, see Figure 1d, which is not observed in the encapsulated devices. Such a peculiar device characteristic in these pristine devices indicates inefficient charge extraction processes, possibly due to the emergence of the energy barrier[25] or a disadvantageous effect due to the time dependent modification of the internal electric field.[26] Both scenarios are essentially a result of the charge accumulation across the interface, prohibiting the movement of charge carriers from perovskite to the HTL. Because in both the competitive devices, the ETL (SnO_2) or ETL/perovskite interface has the least possibility of modification due to the implementation of Al_2O_3 encapsulation, it is logical to ignore any probabilistic effect that may arise from this interface. Upon dark recovery (~72

hrs.), the device recovers its normal trend and the salient S-type feature disappears, as shown in the Figure S5in Supplementary material, which results in a partially-reversible phenomenon. As previously reported, keeping the measured cells under dark conditions allows the redistribution of ions. This paves the understanding that the appearance of the kink in the J-V characteristic is probably due to the non-uniform spatial redistribution of the photo-activated mobile ions that re-appropriates upon relaxation. The temporal modification of the built-in electric field due to ionic accumulation across the interfaces, activated by bias and light, is also evident from the inversion in hysteric effects,[27] which is observed alongside the S-type features. The current-voltage hysteresis usually described in the literature is characterized by higher performance in reverse scan (RS) compared to the forward scan (FS). In Figure S6 a, b in Supplementary material we can see the inversion in hysteresis in J-V curve by the end of 3 hours (180 min), which gets reversed upon relaxation under dark. This concurrently suggests the modification of the built-in electric field in the device due to the incongruous spatial distribution of the photo-activated ions, alongside inappropriate band-alignment. While the inversion in hysteresis in unencapsulated devices is evident, the intensity of the phenomenon is almost invariant in the encapsulated cells along with lesser

hysteresis index in encapsulated devices compared to unencapsulated one as shown in Figure S6c in Supplementary material.

FIG. 2. Variation of hysteretic voltage (ΔV) calculated from dark J-V measurements (shown in Fig S7), the position of cross over points of unencapsulated and encapsulated devices for both the forward and reverse direction with time for 0 min, 30 min, 60 min,120 min ,180 min. In unencapsulated devices the cross over voltage value increase with time means some slow phenomena contributing to this off set. In encapsulated devices the voltage where current is changing direction is almost constant in both directions with measurement time. Slow phenomena that contributing the offset are essentially absent in encapsulated devices.

The adverse effects of mobile ions in the pristine devices are evident even on the dark J-V measurements performed intermittently following the post illumination measurements. The crossover voltage (where, J is minimum) between the forward and the reverse scans, as shown in Figure 2 and the hysteresis Figure S7a-e in Supplementary material for the pristine devices, are found recurrently increasing with time while such changes are essentially absent in the encapsulated devices.

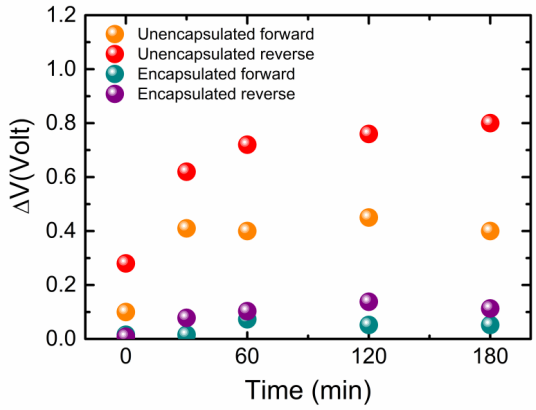

Open circuit voltage decay (OCVD) can be useful to understand the active behavior of the ALD layer, as it provides information on the internal energetics of the devices. These measurements were performed on devices with the same structure under different light soaking conditions (2, 6, and 10 min). Here, the light soaking time is deliberately reduced compared to the previous experiments, avoiding any degradation through an extrinsic

parameter, hence reflecting the effect of the photo-stimulated ions. Our results invariably indicate that the relaxation time constant (τ_{rec}) [28] strictly depends on the illumination time for the pristine devices, as shown Figure S8 a, b in Supplementary material. In contrast, the OCVD and hence the τ_{rec} value remain invariant for the encapsulated devices, as shown in the SI Figure S8 c, d,in Supplementary material (and explanation thereon). Also, the net OCVD is faster in the pristine sample than in comparison to the encapsulated ones that have a sustaining electrostatic potential for a considerably longer time scale, as shown in Figure S8 a, b. Considering the time span of the experiments, the OCVD measurements have little to do with the degradations of the cells; rather, they indicate the effect is also clearly evident in the low frequency capacitance measurements. In this line, frequency dependent capacitance measurements under dark portray a significant change in the electrode polarization,[29,30,31] as shown in Figure SI9in Supplementary material. Prior to any illumination exposure, our measurements reveal that a capacitance value of $7.14 \cdot 10^{-6}$ F/cm^2 at 0.1 Hz for unencapsulated devices, an order of magnitude higher that the encapsulated one, as shown in Figure S9 in Supplementary material. However, the transition frequency (f_s) remains the same in both the devices (ca. 10^1-10^2 Hz) with similar dielectric polarization, while the electrode polarization gets reduced upon Al_2O_3 coating, indicating the better interfacial quality of encapsulated devices. Figure S10a in Supplementary material shows a non-capacitive current under slow-scan rate, indicative of the impact of chemical modification of the perovskite-HTM interface, especially in the pristine devices. Such irreversible non-capacitive effect[32,33] that may originate the permanent degradation of the pristine devices is distinctly absent in the coated devices, as shown in Figure S10b in Supplementary material, probably due to the favorable band alignment at the interface.

We further performed the electrochemical impedance spectroscopy (EIS), under illumination, to gain insight on the underlying mechanisms of these effects. Generally, the

ETL/perovskite interface has a significant influence over the parameters depicted in EIS, partly because the mobility of electrons is much higher.[34] It is evident through literature that in a given system, the charge separation and extraction process is not only influenced by the ETL/perovskite interface but also the perovskite/HTL interface. Here, EIS has measured under AM 1.5 G illumination at open circuit conditions, intermittently along with J-V and results in the characteristic pattern for perovskite solar cells as shown in Figure 3.

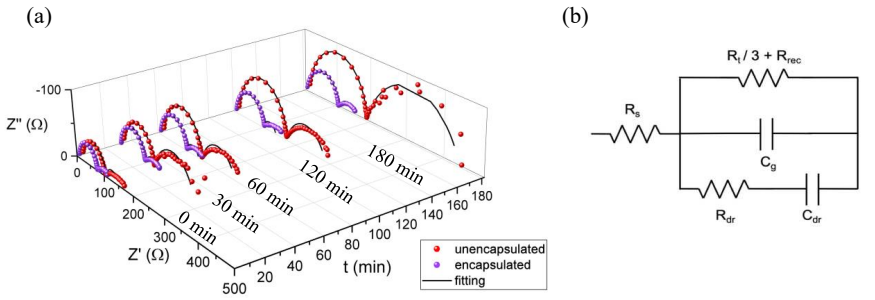

FIG. 3.(a) Nyquist plot measured in light at open circuit condition for unencapsulated (red) and encapsulated (purple) for 0 min, 30 min, 60 min ,120 min ,180 min and (b) the equivalent circuit including Cg is geometrical capacitance, a combination of dielectric relaxation and transport resistance R_t and recombination resistance R_{rec}. The size of two arcs are changing with time in unencapsulated devices as the measurement time progress whereas the size remain almost unchanged in encapsulated devices.

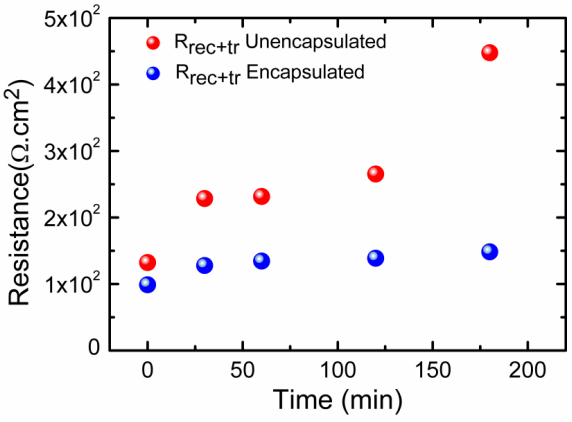

FIG. 4.Variation of combined effect of recombination resistance and charge transfer resistance for unencapsulated (red) and encapsulated (blue) devices with time 0 min,30 min,60 min,120 min,180 min.The value of R_{rec+tr} of unencapsulated devices increases with time but it is almost constant in encapsulated devices .

The impedance spectra are analyzed with an equivalent circuit which consists of a series resistance (R_s) accounting for the purely resistive effects of cables, TCO, etc., a resistor where recombination and charge transport/transfer effects are coupled (R_{rec+tr}), the geometric capacitance of the device (C_g), and a parallel branch, including a capacitor (C_{dr}) and a resistor (R_{dr}) in series.[36] While the rest of the parameters do not show significant changes in time, as shown in Figure S11 in Supplementary material, R_{rec+tr} displays a clear increase, see Figure 4. In particular, R_{rec+tr} increases more abruptly in the unencapsulated case. It is worth to remark that this parameter is obtained from the total resistance of both arcs in the Nyquist plots. It contains the coupled contributions of recombination and a third of charge transport, including that of the selective contacts and interfaces. Although the combinations of different effects in the same resistance hinder the numeric interpretation of the individual components, the feedback obtained from the J-V enables a qualitative characterization of the degradation mechanisms. In our case, the initial effect of the encapsulation is reflected in a slight decrease of the R_{rec+tr}, which is attributed to the increase of the hole selective material conductivity as

shown in Figure S12 in Supplementary material which is well supported by other experimental shreds of evidence. Figure S12 in Supplementary material shows an order of increase in the lateral conductivity of the spiro-OMeTAD upon Al_2O_3 coating. Considering the evolution of the V_{OC}, one would expect the decrease of the recombination resistance to be more intense in the unencapsulated case. Nonetheless, R_{rec+tr} increases with time, which reflects a deterioration of the charge transport characteristics of the device. As evident from FF evolution as well, the encapsulation strongly slows down this process. In this sense, the transport properties deterioration, considering other supporting experimental observations as discussed previously, indicates an increase of the charge transfer resistance at the interface.

Our conclusion is in accord with the similar hypothesis put forwarded by Schulz et al.,[37] who rightfully indicated that the offset between the perovskite-spiro-OMeTAD plays an important role in charge extraction efficiency of that interface. An improper offset that gives rise to inefficient charge extraction has a detrimental effect on device performance. Improved conductivity in the HTM upon ALD alumina deposition essentially implies the increased carrier concentration in the material, and hence, the electronic band-structure is getting modified. Figure S13 in Supplementary material shows an increment of the work function 0.15-0.2 eV upon Al_2O_3 coating from ultraviolet photoelectron spectroscopy (UPS), indicating probabilistic changes in the interfacial (perovskite/spiro-OMeTAD) band structure. The modified interfacial electronic band-structure upon Al_2O_3 coating discourages ion-induced modifications of the interfaces in encapsulated devices. In contrast, for the pristine devices, ion-induced modification of the interface is evident, resulting in inefficient charge extraction and charge carrier accumulation across the perovskite/spiro-OMeTAD interfaces. This ion-induced detrimental modification becomes more severe in the slow scan rate where long polarization is happening, causing chemical degradation, known as the non-capacitive effect.[38] Again the inverted hysteresis, as shown in Figure SI-6, is also a result of the

unfavorable band bending. It was suggested that the accumulated ions under reverse scan might enhance the internal drift field in bulk but generated reversed electric field regions at the interfaces. The inversion of the hysteresis indeed is a fingerprint of the development of the inefficient extraction barrier, due to the change in the local electric field derived from the inappropriate distribution of the mobile ions.

In summary, our experimental observations lead to the conclusion that in the presence of the preferred extraction barrier, the interfacial ion-accumulation is prohibited in the Al_2O_3 coated devices resulting in better intrinsic stability. Significantly, Al_2O_3 produces an active effect in the perovskite layer affecting its behavior beyond the simple passive role supposed for an encapsulation system. Improved conductivity of the spiro-OMeTAD upon Al_2O_3 coating also influences the perovskite-HTL interfacial band structure. Lowering of capacitance in the electrode polarization regime with negligible non-capacitive current and above all, the absence of the s-type kink in the J-V characteristics unequivocally proves the proposed hypothesis. In contrast, for pristine devices the inefficient charge extraction, probably due to temporally varying interfacial electronic-band structure, can be the primal cause that paves to the degradation of the devices. Based on our understanding, we suggest that interface degradation takes place before than the material degradation is initiated. These results pave the way for the development of encapsulation systems that act synergistically on both the active layer performance and the long term stability beyond conventional encapsulation that merely acts as a blocking system, with no direct effect of the working behavior of the active layer.

SUPPLEMENTARY MATERIAL

See supplementary material for full discussion of experimental section.

ACKNOWLEDGEMENTS

The authors thank financial support from the Ministry of New and Renewable Energy, Government of India. S.G. thanks University Grant Commission, Govt. of India for financial support. R.S. thanks German Academic Exchange Service (DAAD) for financial support. Authors thank Neha Mahuli and Bireswar Mandol for their timely help with ALD. P.P.B. would like to thank Ministerio de Economíay Competitividad of Spain for the funding through the project MAT2017-88905-P and his RyC contract; and Generalitat Valenciana (SEJI2017/2017/012).

References:

[1] J.A. McLeod and L. Liu, J. Phys. Chem. Lett. **9**, 2411 (2018).

[2] P. Yadav, D. Prochowicz, E.A. Alharbi, S.M. Zakeeruddin, and M. Grätzel, J. Mater. Chem. C **5**, 7799 (2017).

[3] N.-K. Kim, Y.H. Min, S. Noh, E. Cho, G. Jeong, M. Joo, S.-W. Ahn, J.S. Lee, S. Kim, K. Ihm, H. Ahn, Y. Kang, H.-S. Lee, and D. Kim, Sci. Rep. **7**, 4645 (2017).

[4] M. Salado, L. Contreras-Bernal, L. Caliò, A. Todinova, C. López-Santos, S. Ahmad, A. Borras, J. Idígoras, and J.A. Anta, J. Mater. Chem. A **5**, 10917 (2017).

[5] H.J. Jung, D. Kim, S. Kim, J. Park, V.P. Dravid, and B. Shin, Adv. Mater. **30**, 1802769 (2018).

[6] N. Aristidou, C. Eames, I. Sanchez-Molina, X. Bu, J. Kosco, M. Saiful Islam, and S.A. Haque, Nat. Commun. **8**, (2017).

[7] R. Cheacharoen, N. Rolston, D. Harwood, K.A. Bush, R.H. Dauskardt, and M.D. McGehee, Energy Environ. Sci. **11**, 144 (2018).

[8] L. Shi, T.L. Young, J. Kim, Y. Sheng, L. Wang, Y. Chen, Z. Feng, M.J. Keevers, X. Hao, P.J. Verlinden, M.A. Green, and A.W.Y. Ho-Baillie, ACS Appl. Mater. Interfaces **9**, 25073 (2017).

[9] X. Dong, X. Fang, M. Lv, B. Lin, S. Zhang, J. Ding, and N. Yuan, J. Mater. Chem. A **3**, 5360 (2015).

[10] S. Seo, S. Jeong, C. Bae, N.-G. Park, and H. Shin, Adv. Mater. **30**, 1801010 (2018).

[11] D. Koushik, W.J.H. Verhees, Y. Kuang, S. Veenstra, D. Zhang, M.A. Verheijen, M. Creatore, and R.E.I. Schropp, Energy Environ. Sci. **10**, 91 (2017).

[12] M. V. Khenkin, A. K. M., I. Visoly-Fisher, S. Kolusheva, Y. Galagan, F. Di Giacomo, O. Vukovic, B.R. Patil, G. Sherafatipour, V. Turkovic, H.-G. Rubahn, M. Madsen, A. V. Mazanik, and E.A. Katz, ACS Appl. Energy Mater. **1**, 799 (2018).

[13] C. A. Wilson, R. K. Grubbs, and S. M. George, Chem. Mater. **17**, 5625 (2005).

[14] W. Luo, Y.S. Khoo, P. Hacke, V. Naumann, D. Lausch, S.P. Harvey, J.P. Singh, J. Chai, Y. Wang, A.G. Aberle, and S. Ramakrishna, Energy Environ. Sci. **10**, 43 (2017).

[15] L. Jiang, J. Lu, S.R. Raga, J. Sun, X. Lin, W. Huang, F. Huang, U. Bach, and Y.-B. Cheng, Nano Energy **58**, 687 (2019).

[16] M. De Bastiani, G. Dell'Erba, M. Gandini, V. D'Innocenzo, S. Neutzner, A.R.S. Kandada, G. Grancini, M. Binda, M. Prato, J.M. Ball, M. Caironi, and A. Petrozza, Adv. Energy Mater. **6**, 1501453 (2016).

[17] J. Carolus, T. Merckx, Z. Purohit, B. Tripathi, H.-G. Boyen, T. Aernouts, W. De Ceuninck, B. Conings, and M. Daenen, Sol. RRL **3**,1900226 (2019).

[18] M. V. Khenkin, A. K. M., E.A. Katz, and I. Visoly-Fisher, Energy Environ. Sci. **12**, 550 (2019).

[19] M. V. Khenkin, A. K. M., I. Visoly-Fisher, Y. Galagan, F. Di Giacomo, B.R. Patil, G. Sherafatipour, V. Turkovic, H.-G. Rubahn, M. Madsen, T. Merckx, G. Uytterhoeven, J.P.A. Bastos, T. Aernouts, F. Brunetti, M. Lira-Cantu, and E.A. Katz, Energy Environ. Sci. **11**, 739 (2018).

[20] R. Gottesman, P. Lopez-Varo, L. Gouda, J.A. Jimenez-Tejada, J. Hu, S. Tirosh, A. Zaban, and J. Bisquert, Chem **1**, 776 (2016).

[21] D. Shin, D. Kang, J. Jeong, S. Park, M. Kim, H. Lee, and Y. Yi, J. Phys. Chem. Lett. **8**, 5423 (2017).

[22] C. Ding, Y. Zhang, F. Liu, Y. Kitabatake, S. Hayase, T. Toyoda, K. Yoshino, T. Minemoto, K. Katayama, and Q. Shen, Nano Energy **53**, 17 (2018).

[23] R. Singh, S. Ghosh, A.S. Subbiah, N. Mahuli, and S.K. Sarkar, Sol. Energy Mater. Sol. Cells **205**,110289 (2020).

[24] K. Domanski, B. Roose, T. Matsui, M. Saliba, S.H. Turren-Cruz, J.P. Correa-Baena, C.R. Carmona, G. Richardson, J.M. Foster, F. De Angelis, J.M. Ball, A. Petrozza, N. Mine, M.K. Nazeeruddin, W. Tress, M. Grätzel, U. Steiner, A. Hagfeldt, and A. Abate, Energy Environ. Sci. **10**, 604 (2017).

[25] W. Tress and O. Inganäs, Sol. Energy Mater. Sol. Cells **117**, 599 (2013).

[26] W. Tress, N. Marinova, T. Moehl, S.M. Zakeeruddin, M.K. Nazeeruddin, and M. Grätzel, Energy Environ. Sci. **8**, 995 (2015).

[27] F. Wu, R. Pathak, K. Chen, G. Wang, B. Bahrami, W.-H. Zhang, and Q. Qiao, ACS Energy Lett. **3**, 2457 (2018).

[28] L. Bertoluzzi, R.S. Sanchez, L. Liu, J.-W. Lee, E. Mas-Marza, H. Han, N.-G. Park, I. Mora-Sero, and J. Bisquert, Energy Environ. Sci. **8**, 910 (2015).

[29] O. Almora, I. Zarazua, E. Mas-Marza, I. Mora-Sero, J. Bisquert, and G. Garcia-Belmonte, J. Phys. Chem. Lett. **6**, 1645 (2015).

[30] V.K. Sangwan, M. Zhu, S. Clark, K.A. Luck, T.J. Marks, M.G. Kanatzidis, and M.C. Hersam, ACS Appl. Mater. Interfaces **11**, 14166 (2019).

[31] F. Galatopoulos, A. Savva, I.T. Papadas, and S.A. Choulis, APL Mater. **5**, 076102 (2017).

[32] O. Almora, C. Aranda, I. Zarazua, A. Guerrero, and G. Garcia-Belmonte, ACS Energy Lett. **1**, 209 (2016).

[33] G. Garcia-Belmonte and J. Bisquert, ACS Energy Lett. **1**, 683 (2016).

[34] X. Shi, Y. Ding, S. Zhou, B. Zhang, M. Cai, J. Yao, L. Hu, J. Wu, S. Dai, and M.K. Nazeeruddin, Adv. Sci. 1901213 (2019).

[35] L. Zhou, Y. Zuo, T.K. Mallick, and S. Sundaram, Sci. Rep. **9**, 8778 (2019).

[36] S.-M. Yoo, S.J. Yoon, J.A. Anta, H.J. Lee, P.P. Boix, and I. Mora-Seró, Joule **3**,2535 (2019).

[37] P. Schulz, E. Edri, S. Kirmayer, G. Hodes, D. Cahen, and A. Kahn, Energy Environ. Sci. **7**, 1377 (2014).

[38] J. Carrillo, A. Guerrero, S. Rahimnejad, O. Almora, I. Zarazua, E. Mas-Marza, J. Bisquert, and G. Garcia-Belmonte, Adv. Energy Mater. **6**, 1502246 (2016).

PLEASE CITE THIS ARTICLE AS DOI: 10.1063/1.5144038

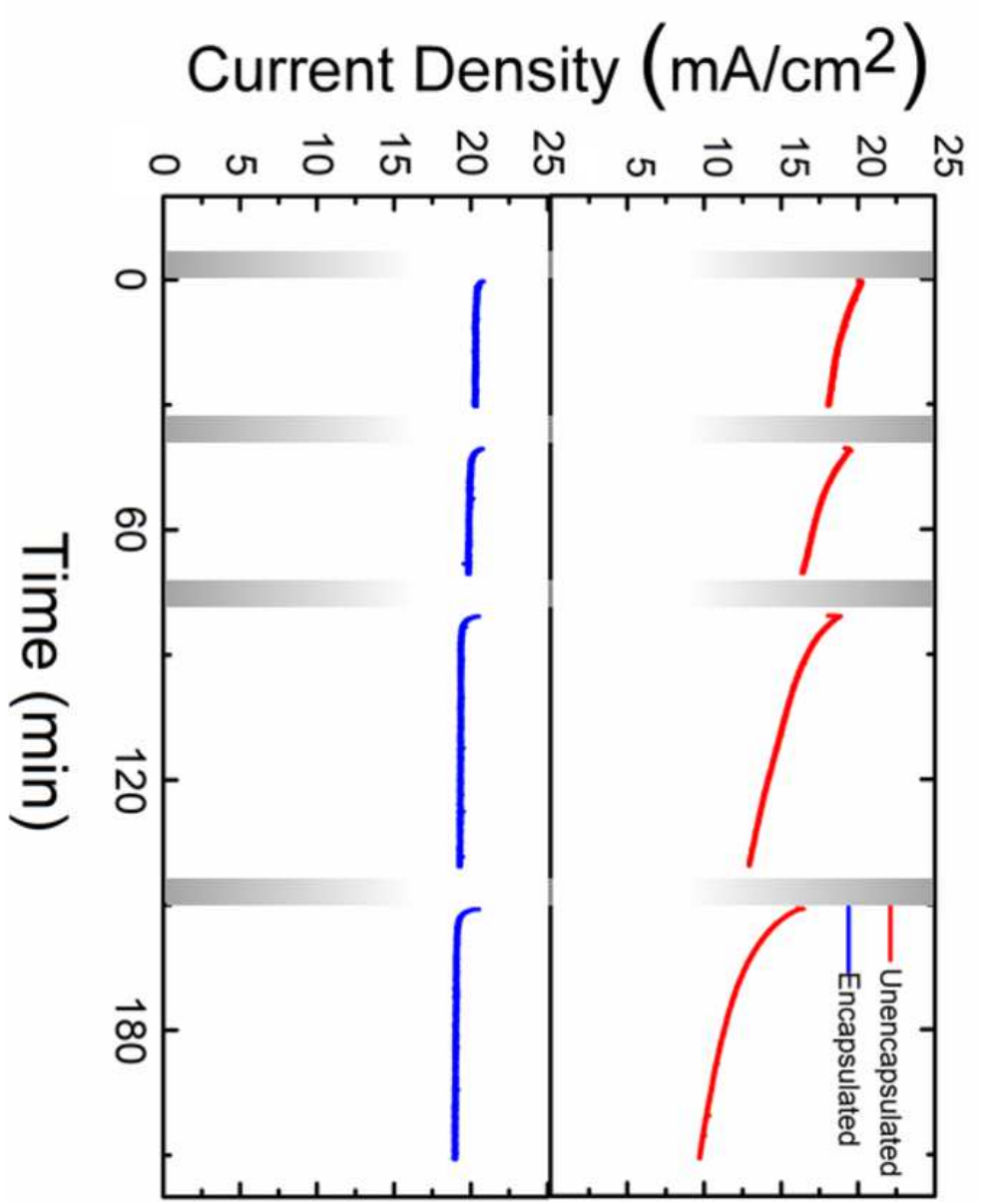

PLEASE CITE THIS ARTICLE AS DOI: 10.1063/1.5144038

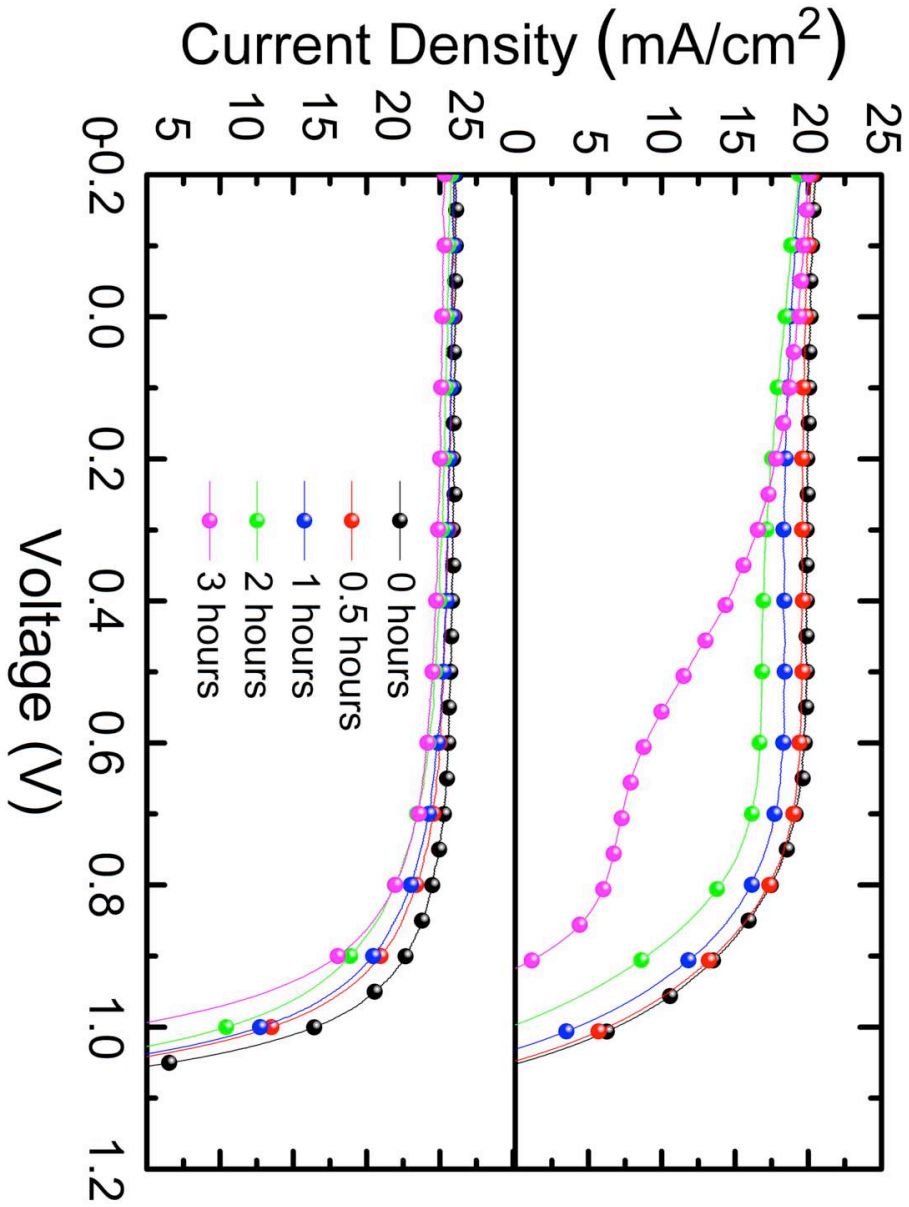

PLEASE CITE THIS ARTICLE AS DOI: 10.1063/1.5144038

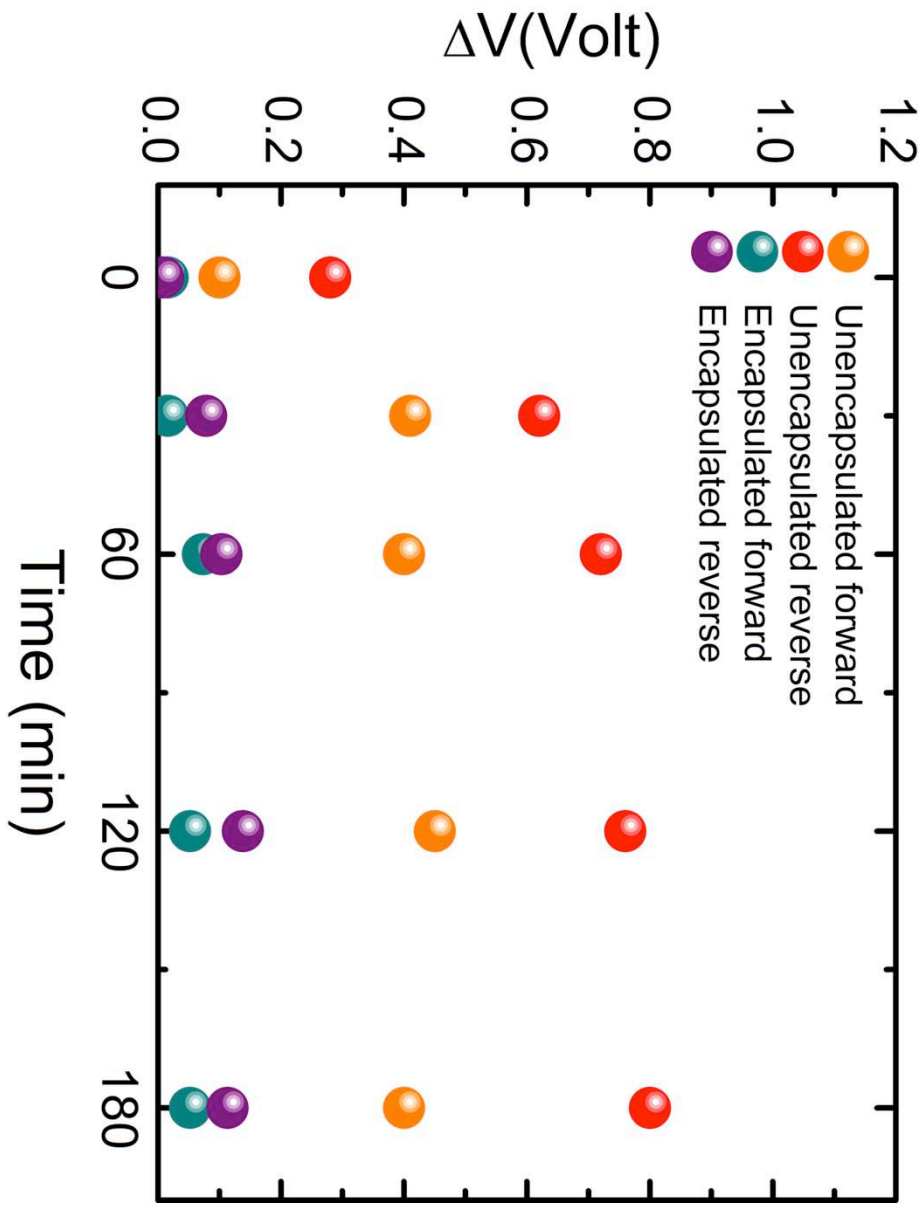

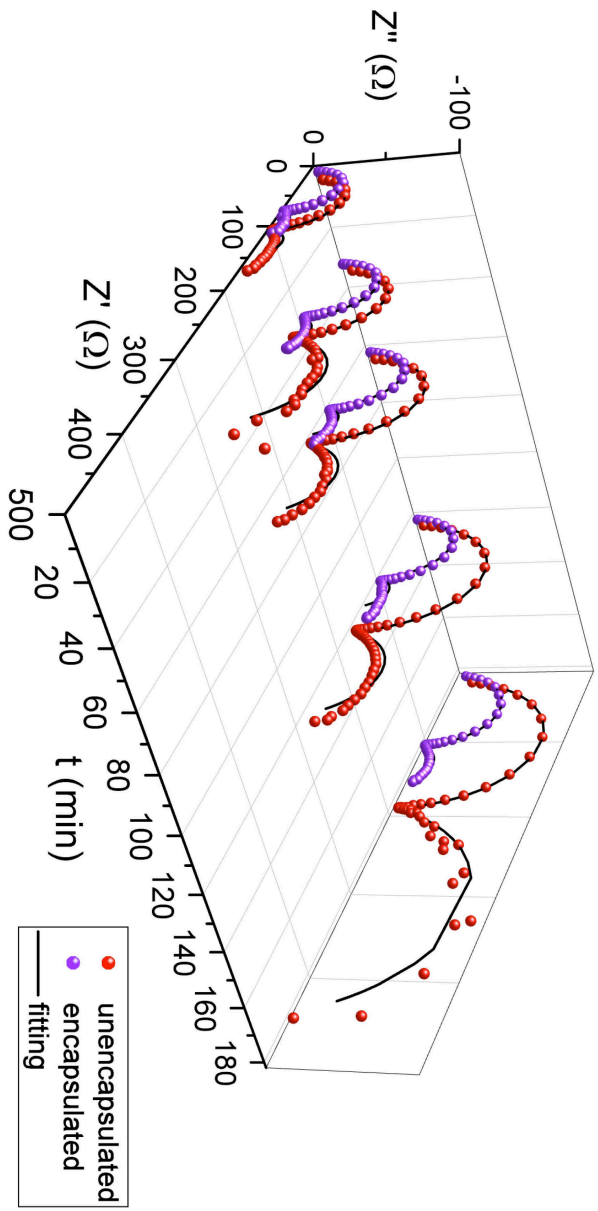

PLEASE CITE THIS ARTICLE AS DOI: 10.1063/1.5144038